A New Technique for the Stable Incorporation of Static Field Solutions in the FDTD Method for the Analysis of Thin Wires and Narrow Strips

Ian J. Craddock and Chris J. Railton, *Member, IEEE*

***Abstract*— The behavior of the fields around many common objects (e.g., wires, slots, and strips) converges to known static solutions. Incorporation of this *a priori* knowledge of the fields into the finite-difference time-domain (FDTD) algorithm provides one method for obtaining a more efficient characterization of these structures. Various methods of achieving this have been attempted; however, most have resulted in unstable algorithms. Recent investigations into the stability of FDTD have yielded criteria for stability, and this contribution for the first time links these criteria to a general finite-element formulation of the method. It is shown that the finite-element formulation provides a means by which FDTD may be generalized to include whatever *a priori* knowledge of the field is available, without compromising stability. Example results are presented for extremely narrow microstrip lines and wires.**

***Index Terms*—Electromagnetic analysis, FDTD methods, finite-element methods, Galerkin method.**

I. Introduction

THE finite-difference time-domain (FDTD) method is well established as a versatile electromagnetic-analysis technique [1]. However, when used to analyze structures with a wide range of dimensions (e.g., those containing microstrip lines and thin wires), a very fine spatial discretization is required to accurately characterize the electrically small features. The resultant increase in the number of FDTD unit cells and the corresponding decrease in the algorithm time step [1] together create vastly increased demands for both storage and computation in the algorithm.

The behavior of the field electrically close to these objects is known; if this *a priori* knowledge of the field behavior was incorporated into the algorithm then there would be less requirement for any increase in spatial resolution. Attempts to accomplish this [2] showed promise, but the modifications required for the FDTD algorithm, while increasing accuracy, compromised stability to the extent that the technique was impractical.

Recently, however, the authors have shown that by considering a passive electrical circuit analog to the FDTD algorithm [3] when formulating a scheme for including *a priori* knowledge of field behavior in the algorithm, the stability properties of the method are retained. In [4], a scheme based on the equivalent circuit for incorporating the known field behavior for microstrip lines with a width of a number of unit cells into the FDTD algorithm was presented.

In this paper, an entirely new and general technique for the inclusion of *a priori* knowledge is presented; this new methodology is developed from the point of view of the finite-element method and is used to extend the work in [4] to narrow microstrip (where the strip width could be less than one unit cell) and to the case of modeling thin wires.

II. FDTD as a Finite-Element Method

It is instructive to consider how the Yee FDTD algorithm can be derived from a finite-element perspective. The general time-domain finite-element formulation can be approached in a number of ways (see [5] for one such alternative formulation), and to present it in full detail and rigor would require a great deal of space—for the purposes of this paper, the theory may be abbreviated and simplified somewhat as follows.

A three-dimensional Cartesian coordinate system is assumed, each component of the electric and magnetic field vectors can be expanded in terms of a suitable set of basis functions, e.g.,

$$H_y(x,y,z,t) = \sum^{i,j,k} H_{y_{i,j,k}}(t)\phi^{H_y}_{i,j,k}(x,y,z)$$
$$E_z(x,y,z,t) = \sum^{i,j,k} E_{z_{i,j,k}}(t)\phi^{E_z}_{i,j,k}(x,y,z) \qquad (1)$$

and so on for the other field components (henceforth, the dependence of the coefficients on the time variable t and the basis functions on x, y, z is assumed and omitted from equations for clarity, for the same reason the summation limits are removed).

The basis functions are assumed to have only local support; the notation used herein conveniently indicates the volume where the function is nonzero by subscripts and superscripts; e.g., the function $\phi^{E_z}_{i,j,k}$ is equal to zero outside a $\Delta \times \Delta \times \Delta$ cubical volume centered on the point $(x = i\Delta, y = j\Delta, z = (k + \frac{1}{2})\Delta)$—in other words, the position of the relevant component in the FDTD unit cell i, j, k (a uniform mesh being assumed for simplicity).

Manuscript received July 25, 1996; revised April 28, 1997. This work was supported by the Defence Research Agency, Malvern, U.K.

The authors are with the Centre for Communications Research, University of Bristol, Bristol BS8 1UB, U.K. (email ian.craddock@bristol.ac.uk; chris.railton@bristol.ac.uk).

Publisher Item Identifier S 0018-9480(98)05511-2.

Introducing these functions and their associated coefficients into Maxwell's curl equations yields

$$-\mu \sum \phi^{H_y}_{i,j,k} \partial_t H_{y_{i,j,k}} = \sum E_{x_{i,j,k}} \partial_z \phi^{E_x}_{i,j,k} - \sum E_{z_{i,j,k}} \partial_x \phi^{E_z}_{i,j,k} \quad (2)$$

$$\epsilon \sum \phi^{E_z}_{i,j,k} \partial_t E_{z_{i,j,k}} = \sum H_{z_{i,j,k}} \partial_x \phi^{H_y}_{i,j,k} - \sum H_{x_{i,j,k}} \partial_y \phi^{H_x}_{i,j,k} \quad (3)$$

where ∂_z, for example, represents partial differentiation with respect to z (a homogeneous, isotropic, and lossless medium has been assumed for clarity; however, the formulation may easily be made more general).

An inner product [6] with each member of a set of test functions is introduced in the usual fashion as follows:

$$-\mu \left\langle \psi_m, \sum \phi^{H_y}_{i,j,k} \right\rangle \partial_t H_{y_{i,j,k}} = \left\langle \psi_m, \sum E_{x_{i,j,k}} \partial_x \phi^{E_x}_{i,j,k} \right\rangle - \left\langle \psi_m, \sum E_{z_{i,j,k}} \partial_x \phi^{E_z}_{i,j,k} \right\rangle \quad \forall \psi_m \quad (4)$$

$$\epsilon \left\langle \psi_m, \sum \phi^{E_z}_{i,j,k} \right\rangle \partial_t E_{z_{i,j,k}} = \left\langle \psi_m, \sum H_{z_{i,j,k}} \partial_x \phi^{H_z}_{i,j,k} \right\rangle - \left\langle \psi_m, \sum H_{x_{i,j,k}} \partial_z \phi^{H_x}_{i,j,k} \right\rangle \quad \forall \psi_m. \quad (5)$$

The test functions are, like the basis functions, assumed to have only local support and the same notation is introduced to denote the $\Delta \times \Delta \times \Delta$ volume over which they are nonzero. This has the effect that most of the inner products become zero, so (4) and (5) may be written (for any given i, j, k) as follows:

$$\mu \langle \psi^{H_y}_{i,j,k}, \phi^{H_y}_{i,j,k} \rangle \partial_t H_{y_{i,j,k}} = -\langle \psi^{H_y}_{i,j,k}, \partial_z \phi^{E_x}_{i,j,k} \rangle E_{x_{i,j,k}} - \langle \psi^{H_y}_{i,j,k}, \partial_z \phi^{E_x}_{i,j,k+1} \rangle E_{x_{i,j,k+1}} + \langle \psi^{H_y}_{i,j,k}, \partial_x \phi^{E_z}_{i,j,k} \rangle E_{z_{i,j,k}} + \langle \psi^{H_y}_{i,j,k}, \partial_x \phi^{E_z}_{i+1,j,k} \rangle E_{z_{i+1,j,k}} \quad (6)$$

$$\epsilon \langle \psi^{E_z}_{i,j,k}, \phi^{E_z}_{i,j,k} \rangle \partial_t E_{z_{i,j,k}} = \langle \psi^{E_z}_{i,j,k}, \partial_x \phi^{H_y}_{i,j,k} \rangle H_{y_{i,j,k}} + \langle \psi^{E_z}_{i,j,k}, \partial_x \phi^{H_y}_{i-1,j,k} \rangle H_{y_{i-1,j,k}} - \langle \psi^{E_z}_{i,j,k}, \partial_y \phi^{H_x}_{i,j,k} \rangle H_{x_{i,j,k}} - \langle \psi^{E_z}_{i,j,k}, \partial_y \phi^{H_x}_{i,j-1,k} \rangle H_{x_{i,j-1,k}}. \quad (7)$$

Similar expressions may be derived for all six field components. The values of the inner products in the equations will depend on the form of the basis and test functions and will clearly vary according to the choices made for these functions. Two obvious choices are: piecewise linear ϕ and Dirac delta ψ and piecewise constant ϕ and piecewise constant ψ, and if the usual staggered centred-difference scheme is used to replace the ∂_t operators in (6) and (7), then either choice yields the traditional FDTD algorithm (although the second choice is perhaps to be preferred, as will be shown in the following sections).

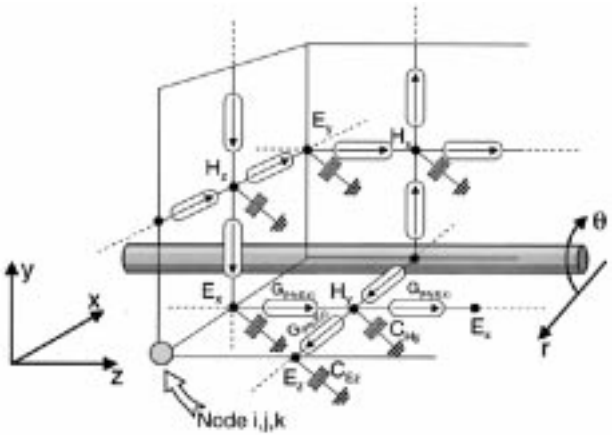

Fig. 1. Section of FDTD mesh and equivalent circuit (including wire).

III. The Equivalent Circuit

The form and application of the FDTD equivalent circuit is described by [3], [4], [7], and [8]. As references to the components of the circuit are needed in later parts of this paper, a brief review is given in this section.

A section of the FDTD mesh and equivalent circuit is illustrated in Fig. 1; considering the *voltage* quantities $H_{y_{i,j,k}}$, $E_{z_{i,j,k}}$, $E_{x_{i,j,k}}$ in unit cell i, j, k and $E_{x_{i,j,k+1}}$ in the adjacent cell, the properties of the gyrators lead to the relationship

$$C_{H_y} \partial_t H_{y_{i,j,k}} = G_{(H_y,E_x)}(E_{x_{i,j,k}} - E_{x_{i,j,k+1}}) - G_{(H_y,E_z)} E_{z_{i,j,k}} \quad (8)$$

and also (neglecting the field components not labeled in Fig. 1)

$$C_{E_z} \partial_t E_{z_{i,j,k}} = G_{(H_y,E_z)} H_{y_{i,j,k}} + \cdots \quad (9)$$

setting all the gyrator values equal to Δ^2 and the capacitor values equal to $\mu\Delta^3$ and $\epsilon\Delta^3$, respectively, gives

$$\partial_t H_{y_{i,j,k}} = \frac{E_{x_{i,j,k}} - E_{x_{i,j,k+1}}}{\mu\Delta} - \frac{E_{z_{i,j,k}}}{\mu\Delta} \quad (10)$$

$$\partial_t E_{z_{i,j,k}} = \frac{H_{y_{i,j,k}}}{\epsilon\Delta} + \cdots \quad (11)$$

and this clearly illustrates the sense in which the circuit is equivalent to the FDTD algorithm. The procedure is simply extended to all the field components (or nodal voltages) and yields the *continuous time* or *semi-discrete* FDTD method (i.e., the time discretization is not included).

It is simple to show [9] that since the equivalent circuit is energy conserving, its continuous time solution is stable (according to any common definition of the term) and, given a central difference approximation to the time derivatives, there is *always* a nonzero value of time step which ensures stability.

The equivalent-circuit concept has been of considerable utility in producing guaranteed stable modified FDTD schemes. In Section IV, the implications of the circuit are considered for the finite-element approach described in the previous section.

IV. Comparison of the Equivalent-Circuit and the Finite-Element Formulation

Comparing the terms in (6) and (8) shows that

$$C_{H_y} = \mu \langle \psi_{i,j,k}^{H_y}, \phi_{i,j,k}^{H_y} \rangle \tag{12}$$

$$G_{(H_y,E_z)} = -\langle \psi_{i,j,k}^{H_y}, \partial_x \phi_{i,j,k}^{E_z} \rangle. \tag{13}$$

Similarly, comparing (7) and (9)

$$G_{(H_y,E_z)} = \langle \psi_{i,j,k}^{E_z}, \partial_x \phi_{i,j,k}^{H_y} \rangle. \tag{14}$$

Thus, for any finite-element formulation of the type assumed in deriving (6) and (7), it is possible to define unique values for the capacitors and gyrators in the equivalent circuit provided that

$$\langle \psi_{i,j,k}^{H_y}, \partial_x \phi_{i,j,k}^{E_z} \rangle = -\langle \psi_{i,j,k}^{E_z}, \partial_x \phi_{i,j,k}^{H_y} \rangle \tag{15}$$

if $\psi_{i,j,k}^{H_y} \equiv \phi_{i,j,k}^{H_y}$ and $\phi_{i,j,k}^{E_z} \equiv \psi_{i,j,k}^{E_z}$ this condition becomes

$$\langle \phi_{i,j,k}^{H_y}, \partial_x \phi_{i,j,k}^{E_z} \rangle = -\langle \phi_{i,j,k}^{E_z}, \partial_x \phi_{i,j,k}^{H_y} \rangle \tag{16}$$

which can be shown to be true by integrating by parts.

To summarize: in formulating a finite-element solution of the type described in Section II, if the basis and test functions are chosen to be identical, then stability, conditional only on the time step, is guaranteed (since the existence of a passive equivalent circuit is guaranteed). Since the standard FDTD algorithm can be derived using piecewise constant test and basis functions, it naturally meets this criterion.

Previous contributions on incorporating *a priori* knowledge into the FDTD algorithm include approaches [10] in which the standard FDTD method was considered basically as a finite-element method with piecewise-linear basis and Dirac delta test functions; the basis functions were modified to more closely match the expected field distributions. These methods often did not result in stable algorithms, as they did not meet the above stability criterion.

The following sections illustrate how *a priori* knowledge of the field close to thin wires and narrow metal strips may be included in the FDTD method by modifying the basis functions. A full description of the formulations in each case would be extremely lengthy—the method is described here for only a few field components (the entire method can be obtained by following the same procedure using the appropriate basis functions and limits of integration in each case).

V. Formulation for Thin Wires

Consider a thin wire with radius a (less than half-a-unit cell dimension), as shown in Fig. 1. The static solutions for the E_z and H_y field components are

$$E_z(r) \propto \ln\left(\frac{r}{a}\right), \qquad r > a \tag{17}$$

$$H_y(r,\theta) \propto \frac{\cos\theta}{r}, \qquad r > a \tag{18}$$

in order to improve the accuracy of the FDTD solution the basis functions in the vicinity of the wire are modified in order that their shape matches these solutions as closely as possible—thus, the basis functions centred on the field components E_z and H_y in Fig. 1 are chosen to be

$$\phi^{H_y}(r,\theta) = \frac{H_y(r,\theta)}{H_y\left(\frac{\Delta}{2},0\right)} \tag{19}$$

$$\phi^{E_z}(r) = \frac{E_z(r)}{E_z(\Delta)} \tag{20}$$

where the functions have been normalized to unity at the position of the two field components.

As shown in previous sections, in this formulation the capacitor values are equal to the inner product between each basis function and itself and the gyrator values to the inner product between each basis function and every other basis function.

For example, the capacitor associated with H_y can be calculated by the integral

$$C_{H_y} = 2\mu\left(\int_0^{\Delta}\int_{\pi/4}^{\pi/2}\int_a^{\Delta/(2\sin\theta)} (\phi^{H_y}(r,\theta))^2\, r\, dr\, d\theta\, dz\right) + 2\mu\left(\int_0^{\Delta}\int_0^{\pi/4}\int_a^{\Delta/(\cos\theta)} (\phi^{H_y}(r,\theta))^2\, r\, dr\, d\theta\, dz\right) \tag{21}$$

and the gyrator linking the H_y and E_z field components is given by (employing now, for convenience a Cartesian coordinate system with an origin at the position of the cell vertex) the integral

$$G_{(H_y,E_z)} = \int_0^{\Delta}\int_{-\Delta/2}^{\Delta/2}\int_{-\infty}^{\infty} (\partial_x \phi^{E_z})\phi^{H_y}\, dx\, dy\, dz. \tag{22}$$

In evaluating this expression it is important to recall that the basis function for E_z must be truncated, normally at $x = \Delta/2$, according to the constraints on the finite-element formulation given in Section II and, on the truncation plane, its x-derivative is a Dirac delta function δ^{E_z} with a weight equal to the discontinuity. In this case, the procedure is modified slightly due to the fact that the adjacent field component is in the wire and, hence, unused—ϕ^{E_z} is accordingly truncated instead at $x = \Delta$.

The integral is then split into the following two parts:

$$G_{(H_y,E_z)} = \int_0^{\Delta}\int_{-\Delta/2}^{\Delta/2}\int_{-\Delta/2}^{\Delta^-} (\partial_x \phi^{E_z})\, \phi^{H_y}\, dx\, dy\, dz + \int_0^{\Delta}\int_{-\Delta/2}^{\Delta/2}\int_{-\infty}^{\infty} \delta^{E_z}(x-\Delta)\, \phi^{H_y}\, dx\, dy\, dz \tag{23}$$

where Δ^- indicates the end of the interval immediately before the discontinuity in ϕ^{E_z}. Integrating the second term with respect to x yields

$$G_{(H_y,E_z)} = \int_0^{\Delta}\int_{-\Delta/2}^{\Delta/2}\int_{-\Delta/2}^{\Delta^-} (\partial_x \phi^{E_z})\, \phi^{H_y}\, dx\, dy\, dz + \int_0^{\Delta}\int_{-\Delta/2}^{\Delta/2} \phi^{E_z}(\Delta)\, \phi^{H_y}(\Delta)\, dy\, dz \tag{24}$$

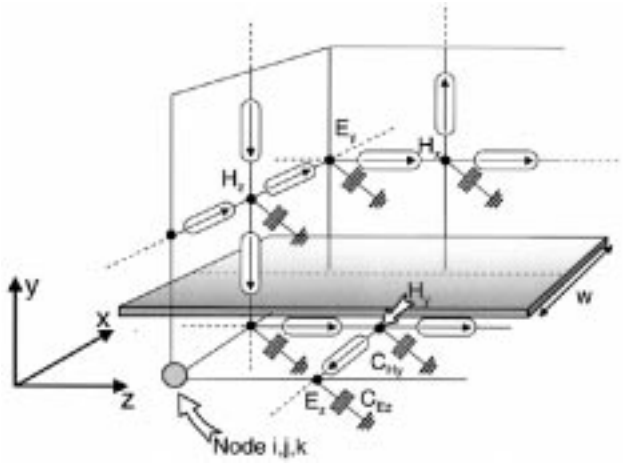

Fig. 2. Section of FDTD mesh and equivalent circuit (including microstrip).

due to the particular form of ϕ^{H_y} (given by [18]), the second integrand is zero and, apart from at the discontinuity, it is easily shown that $\partial_x \phi^{E_z} = \phi^{H_y}$, therefore,

$$G_{(H_y,E_z)} = \int_0^{\Delta} \int_{-\Delta/2}^{\Delta/2} \int_{-\Delta/2}^{\Delta^-} (\phi^{H_y})^2 \, dx \, dy \, dz. \tag{25}$$

The integrals are readily performed numerically at the beginning of the FDTD execution to yield modified update equations based, for example, on (6) and (7). Since the basis functions have been changed to fit the expected field distribution, an improvement in accuracy for any given unit cell size is expected; results obtained using this technique are given in Section VII and confirm that this is the case.

VI. Formulation for Narrow Microstrip

The methodology described in previous sections is, as stated, entirely general. In order to improve the accuracy of FDTD's analysis of narrow microstrip lines, it is simply necessary to choose as the basis functions the known static solutions for the situation, as illustrated in Fig. 2.

In order to proceed, the static solutions for the fields adjacent to a strip of width w are needed—firstly, the following quantities are defined:

$$v(x,y) = y + jx \tag{26}$$

$$p(x,y,w) = \sqrt{\frac{w}{v(x,y)^2 + \left(\frac{w}{2}\right)^2}} \tag{27}$$

$$q(x,y,w) = \sqrt{w} \ln \left(\frac{\frac{w}{2}}{v(x,y) + \sqrt{v(x,y)^2 + \left(\frac{w}{2}\right)^2}} \right) \tag{28}$$

using these quantities and with the x, y origin taken to be the center of the strip, the behavior of the transverse field components is

$$H_x(x,y) \propto E_y(x,y) \propto \frac{p(x,y,w) + p^*(x,y,w)}{2} \tag{29}$$

$$E_x(x,y) \propto H_y(x,y) \propto \frac{p(x,y,w) - p^*(x,y,w)}{2j} \tag{30}$$

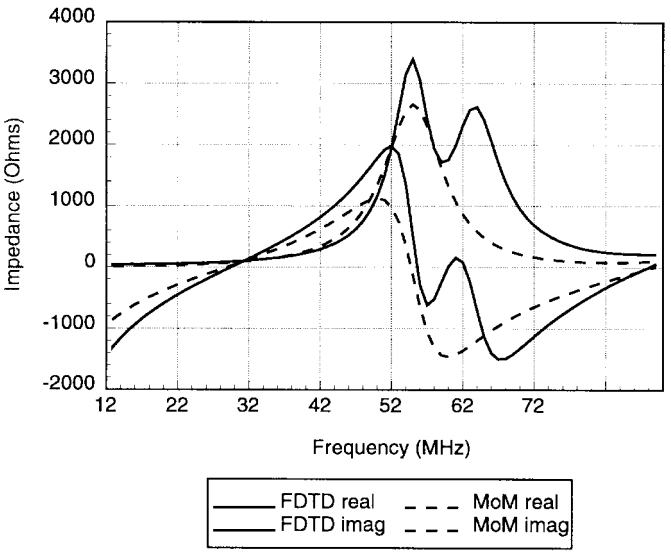

Fig. 3. Input impedance of a 5-m dipole with 1-mm thickness.

(* denoting complex conjugation) and the longitudinal components are given by

$$E_z(x,y) \propto \frac{q(x,y,w) + q^*(x,y,w)}{2} \tag{31}$$

$$H_z(x,y) \propto \frac{q(x,y,w) - q^*(x,y,w)}{2j}. \tag{32}$$

Normalized to unity at the position of the relevant field components, these field solutions can be used to define the basis functions for the field components adjacent to the strip in the same manner as for the thin wires in Section V.

The value of $C_{H_y} = \mu \langle \phi^{H_y}, \phi^{H_y} \rangle$ is, for example, given by

$$C_{H_y} = \mu \int_0^{\Delta} \int_{-\Delta/2}^{\Delta/2} \int_0^{\Delta} (\phi^{H_y})^2 \, dx \, dy \, dz. \tag{33}$$

Due to singularities in the static field solutions, care must be taken with their integration—typically, the integrand is expressed as the sum of singular and nonsingular parts; the singular part is integrated analytically and the nonsingular portion is numerically integrated.

The results obtained using this method for a microstrip line are given in Section VIII.

VII. Results for Thin Wires

To demonstrate that modifying the basis/test functions produces an improvement in accuracy over the standard FDTD method, wire dipoles of 5-m length and with radii between 1 mm and 5 cm were analyzed on an FDTD mesh with 50-cm cell dimension. After exciting the dipoles with a delta-gap source over a wide frequency range, the input impedance was calculated.

As the dipole radius was at all times less than the FDTD unit cell size, the standard FDTD algorithm would have predicted the same input impedance regardless of the value of radius. Figs. 3–6 compare the results using the modified basis functions with FDTD and a well-proven wire dipole method

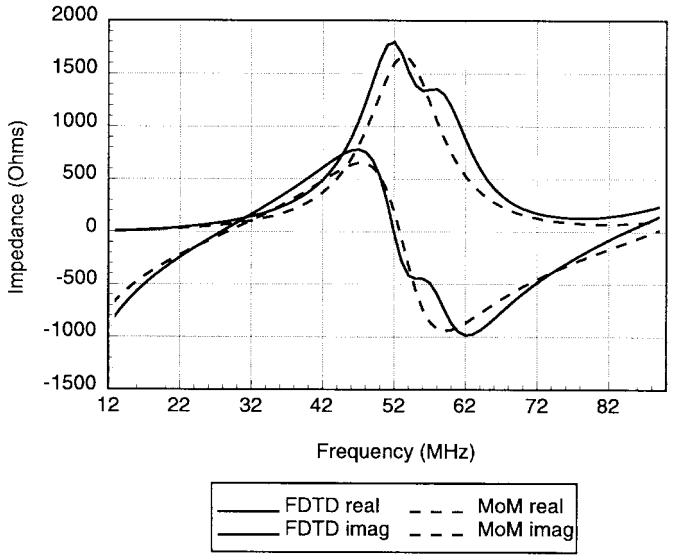

Fig. 4. Input impedance of a 5-m dipole with 10-mm thickness.

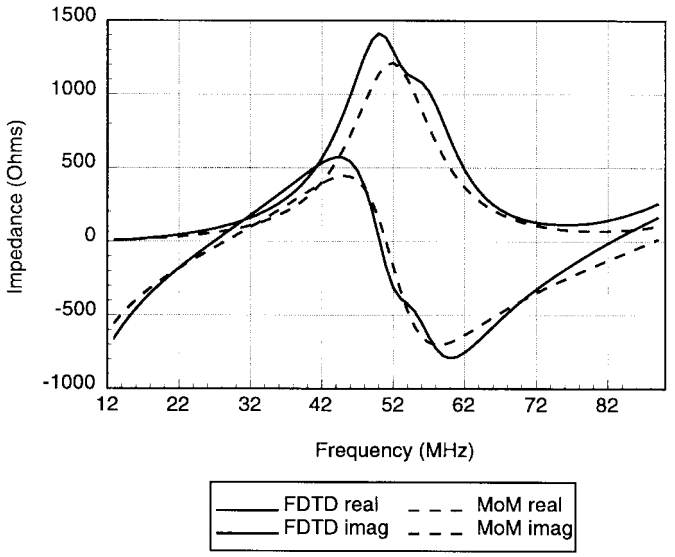

Fig. 5. Input impedance of a 5-m dipole with 20-mm thickness.

of moments (MoM) technique employing piecewise sinusoidal basis functions [11].

In each case, the dipole radius is much less than the FDTD unit cell size; however, the change in impedance as a function of radius and frequency closely matches the MoM technique. The dips in the calculated impedance values at 60 MHz for the cases of extremely small radii were found to be phenomena arising from the longitudinal discretization of the dipole problem rather than the (radial) modified basis functions.

All cases were entirely stable with a choice of time step equal to the standard value for a three-dimensional FDTD problem.

VIII. Results for Narrow Microstrip

In order to validate the application of the method to a narrow strip, as described in Section VI, the variation in effective

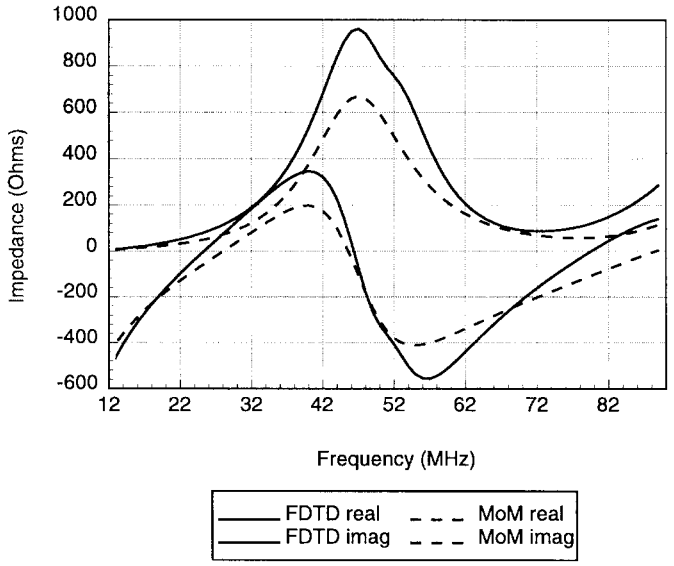

Fig. 6. Input impedance of a 5-m dipole with 50-mm thickness.

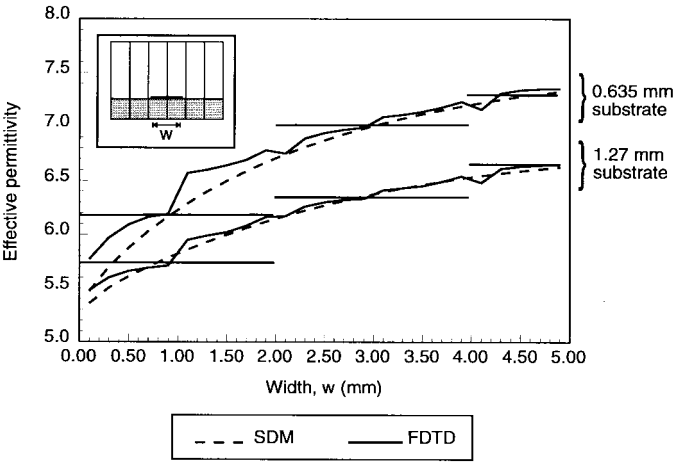

Fig. 7. Dispersion characteristics of boxed microstrip lines ($\epsilon_r = 8.875$).

permittivity of a boxed microstrip structure was sought over frequency.

Two different FDTD models were investigated, each one using modified basis functions to achieve an accurate characterization of the effective permittivity. These models were: 0.635-mm substrate thickness, 0.3175-mm unit cell height and 1.270-mm substrate thickness, 0.3175-mm unit cell height.

The substrate relative permittivity was 8.875 and the width of the strip was altered from a small fraction of the transverse unit cell size (equal to 1 mm) to almost five unit cells. Fig. 7 shows the calculated effective permittivities at a spot frequency of 2 GHz.

The dashed lines in Fig. 7 were produced using a spectral-domain method (SDM), which is capable of highly accurate characterizations of microstrip structures [12]. The continuous solid lines are the results generated using the modified basis functions and the discontinuous horizontal lines were the values calculated using a standard FDTD method.

Clearly the standard FDTD algorithm is unable to resolve subcellular changes in strip width and, except at the single

points where (essentially by coincidence) the lines intersect the true curves, the effective permittivities obtained vary widely from the correct values. In contrast, the method described in Section VI follows the SDM results closely even when the strip width is a small fraction of a unit cell.

In both the modified and standard FDTD methods, it is apparent that the vertical discretization through the substrate plays an important part in accurately modeling the microstrip, the models employing four unit cells here produce better results.

The accuracy of the results presented here is similar to that achieved in [13] using an alternative technique for incorporating the static field solution. However, the formulation used in this contribution has the advantage of resulting in a stable algorithm.

IX. Conclusions

FDTD may be formulated as a time-domain finite-element method; one method to improve its accuracy without increasing its computational overheads is to modify the basis functions in order to match the known field behavior close to wires, strips, etc. In general, however, the modifications to the basis functions may very easily result in instability and render the algorithm unusable.

This contribution, by examining the correspondence between the finite-element formulation and the FDTD equivalent circuit, has shown that finite-element schemes, if they use identical basis and test functions, will be stable.

Formulations which incorporate modified basis functions for thin wires and narrow microstrip lines have been presented and, by applying these to a number of example problems, it has been demonstrated that they provide not only stable algorithms, but ones which do indeed improve the accuracy of analysis significantly.

In addition to the clear practical uses of the techniques described herein, it is felt that the very different, yet entirely complementary, insights offered by the equivalent-circuit and finite-element viewpoints will be of interest and value to workers in this area.

Acknowledgment

The authors would like to thank Prof. J. P. McGeehan for provision of facilities at the Centre for Communications Research, University of Bristol, Bristol, U.K.

References

[1] K. S. Kunz and R. J. Luebbers, *The Finite Difference Time Domain Method for Electromagnetics*. Boca Raton, FL: CRC Press, 1993.

[2] D. B. Shorthouse and C. J. Railton, "Incorporation of static singularities into the finite difference time domain technique with application to microstrip structures," in *Proc. 20th European Microwave Conf.*, Budapest, Hungary, Sept. 1990, pp. 531–536.

[3] I. J. Craddock, C. J. Railton, and J. P. McGeehan, "Derivation and appliation of an equivalent passive circuit for the FDTD algorithm," *Microwave Guided Wave Lett.*, vol. 6, pp. 40–43, Jan. 1996.

[4] I. J. Craddock and C. J. Railton, "Stable inclusion of *a priori* knowledge in the FDTD algorithm: Application to microstrip lines," in *Proc. IEEE AP-S/URSI Symp.*, vol. 2, Baltimore, MD, July 1996, pp. 1300–1303.

[5] M. Krumpholtz, C. Huber, and P. Russer, "A field theoretical comparison of FDTD and TLM," *IEEE Trans. Microwave Theory Tech.*, vol. 43, pp. 1935–1950, Aug. 1995.

[6] G. Helmberg, *Introduction to Spectral Theory in Hilbert Space*. New York: Wiley, 1969.

[7] C. J. Railton, I. J. Craddock, and J. B. Schneider, "Improved locally distorted CPFDTD algorithm with provable stability," *Electron. Lett.*, vol. 31, pp. 1585–1586, Aug. 1995.

[8] C. J. Railton and I. J. Craddock, "Analysis of general 3D PEC structures using an improved CPFDTD algorithm," *Electron. Lett.*, vol. 31, pp. 1753–1754, Sept. 1995.

[9] I. J. Craddock and C. J. Railton, "Application of a circuit-based approach to ensuring the stability of modified finite difference time domain algorithms," in *Proc. 12th Int. Zurich Symp. EMC*, Zurich, Switzerland, Feb. 1997, pp. 515–518.

[10] C. J. Railton, "Use of static field solutions in the FDTD method for the efficient treatment of curved metal surfaces," *Electron. Lett.*, vol. 29, pp. 1466–1467, Aug. 1993.

[11] G. A. Thiele, "Wire antennas," in *Computer Techniques for Electromagnetics*, R. Mittra, Ed. New York: Pergamon, 1973.

[12] S. A. Meade and C. J. Railton, "Efficient implementation of the spectral domain method including pre-calculated basis functions," in *Proc. IEEE MTT-S Symp.*, Atlanta, GA, 1993, pp. 991–994.

[13] C. J. Railton, "Modeling of narrow microstrip lines using the FDTD method," *Electron. Lett.*, vol. 28, pp. 1168–1170, June 1992.

Ian J. Craddock was born in the West of England, U.K., in 1972. He received the B.Eng. degree in electronics and communications engineering and the Ph.D. degree from the University of Bristol, Bristol, U.K., in 1992 and 1996, respectively.

He is currently engaged in teaching and research in the Department of Electronic Engineering, University of Bristol, where his interests include the application of time-domain finite-difference, finite-element and finite-volume methods in electromagnetics, and the design and analysis of planar antenna structures and techniques for time-domain field visualization.

Chris J. Railton (M'88) received the B.Sc. degree in physics with electronics from the University of London, London, U.K., in 1974, and the Ph.D. degree in electronic engineering from the University of Bath, Bath, U.K., in 1988.

From 1974 to 1984, he was in the scientific civil service, where he worked on a number or research and development projects in the areas of communications, signal processing, and electromagnetic compatibility (EMC). From 1984 to 1987 he was at the University of Bath, where he was involved with the mathematical modeling of boxed microstrip circuits. He is currently with the Centre for Communications Research, University of Bristol, Bristol, U.K., where he leads the Computational Electromagnetics Group, which is involved in the development of new algorithms and their application to monolithic microwave integrated circuits (MMIC's), planar antennas, microwave and radio-frequency (RF) heating, electromagnetic compatibility (EMC), and high-speed logic.